

Functional equivalence of the transcription factors Pax2 and Pax5 in mouse development

Maxime Bouchard, Peter Pfeffer and Meinrad Busslinger*

Research Institute of Molecular Pathology, Dr Bohr-Gasse 7, A-1030 Vienna, Austria

*Author for correspondence (e-mail: busslinger@nt.imp.univie.ac.at)

Accepted 9 June; published on WWW 9 August 2000

SUMMARY

Pax2 and *Pax5* arose by gene duplication at the onset of vertebrate evolution and have since diverged in their developmental expression patterns. They are expressed in different organs of the mouse embryo except for their coexpression at the midbrain-hindbrain boundary (MHB), which functions as an organizing center to control midbrain and cerebellum development. During MHB development, *Pax2* expression is initiated prior to *Pax5* transcription, and *Pax2*^{-/-} embryos fail to generate the posterior midbrain and cerebellum, whereas *Pax5*^{-/-} mice exhibit only minor patterning defects in the same brain regions. To investigate whether these contrasting phenotypes are caused by differences in the temporal expression or biochemical activity of these two transcription factors, we have generated a knock-in (ki) mouse, which expresses a *Pax5* minigene under the control

of the *Pax2* locus. Midbrain and cerebellum development was entirely rescued in *Pax2*^{5ki/5ki} embryos. *Pax5* could furthermore completely substitute for the *Pax2* function during morphogenesis of the inner ear and genital tracts, despite the fact that the *Pax5* transcript of the *Pax2*^{5ki} allele was expressed only at a fivefold lower level than the wild-type *Pax2* mRNA. As a consequence, the *Pax2*^{5ki} allele was able to rescue most but not all *Pax2* mutant defects in the developing eye and kidney, both of which are known to be highly sensitive to *Pax2* protein dosage. Together these data demonstrate that the transcription factors *Pax2* and *Pax5* have maintained equivalent biochemical functions since their divergence early in vertebrate evolution.

Key words: Pax2/5, Gene substitution, Midbrain, Eye, Ear, Kidney development, Mouse

INTRODUCTION

The duplication of developmental control genes has been a driving force in evolution to increase the diversity and complexity of higher eukaryotes. One of these multigene families codes for the Pax transcription factors, which can be divided into four distinct subclasses based on their sequence similarities (Noll, 1993; Mansouri et al., 1996). The vertebrate *Pax2*, *Pax5* and *Pax8* genes constitute one such subclass, which has been even further diversified during zebrafish evolution by a recent *Pax2* gene duplication (Pfeffer et al., 1998). The genome of most invertebrates, however, contains only a single *Pax2/5/8* gene (Czerny et al., 1997; Fu and Noll, 1997; Wada et al., 1998; Kozmik et al., 1999), indicating that the complexity of this Pax subfamily has arisen by gene duplications at the onset of vertebrate evolution.

Structure-function analyses revealed that the mammalian Pax2, Pax5 and Pax8 proteins possess similar biochemical activities. For instance, the DNA-binding specificity of these proteins is highly similar due to extreme sequence conservation of the N-terminal paired domain (Adams et al., 1992; Kozmik et al., 1993; Czerny et al., 1997). All three proteins, furthermore, contain a conserved transactivation domain at the C terminus (Dörfler and Busslinger, 1996; Lechner and Dressler, 1996) as well as a partial homeodomain, which

constitutes an interaction surface for the retinoblastoma (Rb) and TATA-binding (TBP) proteins (Eberhard and Busslinger, 1999). The three Pax proteins are also able to negatively regulate gene transcription by utilizing a conserved octapeptide motif for recruitment of Groucho corepressor proteins (Eberhard et al., 2000).

The *Pax2*, *Pax5* and *Pax8* genes are expressed in a spatially and temporally overlapping manner at the midbrain-hindbrain boundary (MHB) and in the spinal cord of the mouse embryo (Nornes et al., 1990; Plachov et al., 1990; Adams et al., 1992; Asano and Gruss, 1992). Outside the CNS, *Pax2* and *Pax8* are coexpressed only in the mesenchymal aggregates and derived tubular structures of the developing kidney (Dressler et al., 1990; Plachov et al., 1990). The *Pax2* gene is uniquely expressed in most tissues of the developing urogenital system as well as during eye and inner ear development (Dressler et al., 1990; Nornes et al., 1990), *Pax5* during B-lymphopoiesis (Adams et al., 1992) and *Pax8* in the developing thyroid gland (Plachov et al., 1990). Consistent with these expression patterns, targeted gene inactivation resulted in severe phenotypes, primarily in the unique expression domains of these Pax genes. The loss of *Pax2* results in pathfinding defects of the optic nerve, extension of the pigmented retina into the optic stalk and lack of optic fissure closure during eye development, in the absence of kidney, ureter and genital tracts

in the urogenital system and in agenesis of the cochlea in the developing inner ear (Torres et al., 1995, 1996; Favor et al., 1996). Mice lacking *Pax5* fail to develop B-lymphocytes (Urbánek et al., 1994), which reflects the inability of hematopoietic progenitor cells to undergo B-lineage commitment in the absence of *Pax5* (Nutt et al., 1999). Conversely, the thyroid gland of *Pax8*-deficient mice is devoid of follicular cells (Mansouri et al., 1998).

Individual *Pax* gene mutations, however, show only variable (*Pax2*^{-/-}), mild (*Pax5*^{-/-}) or no (*Pax8*^{-/-}) effects in development of the midbrain and cerebellum, both of which are derived from a common expression domain of these *Pax* genes at the midbrain-hindbrain boundary (MHB) of the embryo (Urbánek et al., 1994; Torres et al., 1996; Mansouri et al., 1998). Interestingly, the severity of the phenotype correlates with the temporal onset of *Pax* gene expression in this brain region. *Pax2* transcription is already initiated in the prospective MHB region during late gastrulation (at day 7.5) (Rowitch and McMahon, 1995), followed by *Pax5* expression at the 3- to 5-somite stage (day 8.25) (Urbánek et al., 1994) and *Pax8* expression at approx. 9 somites (day 8.5) (Pfeffer et al., 1998). Surprisingly, the *Pax2* mutant phenotype is strongly influenced by the genetic background of the mouse strain analyzed, as it can range from complete deletion of the posterior midbrain and cerebellum in the C3H/He strain (Favor et al., 1996) to almost normal development of these brain structures on the C57BL/6 background (Schwarz et al., 1997). In contrast, the posterior midbrain and cerebellum were consistently deleted in *Pax2*, *Pax5* double-mutant embryos regardless of their genetic background (Schwarz et al., 1997). Moreover, progressive inactivation of *Pax2* and *Pax5* alleles resulted in increasing loss of the midbrain and cerebellum, indicating that these two transcription factors cooperatively regulate MHB development in a dosage-dependent manner (Urbánek et al., 1997).

The analysis of double-mutant mice thus suggested that *Pax2* and *Pax5* fulfil similar functions during midbrain and cerebellum development. In apparent contradiction to this hypothesis, we have recently demonstrated a hierarchical relationship between these two transcription factors. *Pax2* was shown to directly bind to and thereby activate the MHB-specific enhancer of the *Pax5* gene (Pfeffer et al., 2000). Furthermore, both *Pax* genes are expressed in a contrasting manner at the MHB. The expression of *Pax2* is initially activated in a broad domain of the prospective MHB region and is later restricted to a narrow stripe centered at the MHB (Rowitch and McMahon, 1995), whereas the expression of *Pax5* is activated later but then persists longer in a relatively broad domain on either side of the MHB (Adams et al., 1992; Asano and Gruss, 1992). The question therefore arises whether the function of these two *Pax* proteins is determined by their difference in spatiotemporal expression or biochemical activity. To address this question, we have inserted a *Pax5* minigene into the *Pax2* locus. Analysis of homozygous knock-in mice on the nonpermissive C3H/He strain background revealed that the development of the midbrain and cerebellum was entirely normal. Hence, the *Pax5* protein can functionally substitute for *Pax2*, indicating that the difference between the two genes stems from their divergent expression patterns during MHB development. *Pax5* was furthermore able to rescue the *Pax2* mutant phenotype in the developing eye, ear

and urogenital system, where the endogenous *Pax5* gene is not expressed. These data therefore demonstrate that the transcription factors *Pax2* and *Pax5* have maintained equivalent biochemical functions since their divergence at the onset of vertebrate evolution.

MATERIALS AND METHODS

Generation of *Pax2*^{5ki} mutant mice

The targeting vector was assembled in pSP64 containing a polylinker with appropriate *loxP* and restriction sites. A 6.5-kb *SpeI*-*BspEI* fragment containing *Pax2* exon 1 and a 1.7-kb *NcoI* fragment from intron 2 were inserted as homology arms, and mouse *Pax5* cDNA was fused at a common *NcoI* site to *Pax2* exon 2. A floxed cassette containing the *HSV-tk* (negative selection) and *tk-neo* (positive selection) genes and a 3.7-kb *BamHI* fragment containing the *lacZ* gene of pGNA-*Pax5* (Urbánek et al., 1994) were inserted downstream of the *Pax5* minigene. *AscI*-linearized DNA (15 µg) of the targeting vector was electroporated into E14.1 ES cells (1×10⁷), followed by selection with 350 µg/ml G418. Individual clones were screened for homologous recombination by nested PCR, using primers in the *lacZ* gene and *Pax2* intron 2, followed by Southern blot analysis of *BsmI*-digested DNA with the *NcoI*-*BsmI* probe 'a'. Cells (1×10⁷) of one correctly targeted clone were electroporated with pMC-Cre (3 µg) followed by selection with 2 µM gancyclovir. Deletion of the selection cassette was monitored by nested PCR, using primers in *Pax2* intron 1 and the *lacZ* gene, and was confirmed by Southern blot analysis of *SacI*-digested DNA with the *SacI*-*BspEI* probe 'b'. This clone was injected into C57BL/6 blastocysts, and chimeric males were mated with C3H/He females followed by back-crossing of the *Pax2*^{5ki} allele into the C3H/He background for five generations.

Histological and immunohistochemical analyses

Embryos or dissected organs were fixed in 4% paraformaldehyde/PBS, and Hematoxylin, Eosin or Nissl staining was performed on 16 µM paraffin-embedded sections. Cryosectioning and immunohistochemical analyses (Matise and Joyner, 1997) were performed with rabbit anti-N-CAM (1:100 dilution), goat anti-E-cadherin (Santa Cruz; 1:100) and rabbit anti-phosphoH3 antibodies (Upstate Biotechnology, 1:200). These antibodies were detected with FITC-labeled donkey anti-rabbit IgG (Santa Cruz; dilution 1:200), biotinylated donkey anti-goat IgG (Santa Cruz; 1:100) detected with Texas Red-coupled avidin (Vector Labs, 1:200) and biotinylated goat anti-rabbit IgG detected by DAB staining with the Vectastain ABC kit (Vector Labs), respectively.

β-galactosidase and TUNEL staining

Embryos were stained for β-galactosidase activity as described (Pfeffer et al., 2000). TUNEL assays were performed on paraffin-embedded sections using the fluorescein in situ cell death detection kit (Roche).

Western blot analysis

Whole cell extracts of 18.5-day-old kidneys were prepared by homogenization in buffer A and analyzed by SDS-PAGE and western blotting as described (Eberhard et al., 1999).

RNase protection assay

RNase protection analysis (Urbánek et al., 1994) was performed with riboprobes, which were derived from *Pax2*^{5ki/+} kidney by RT-PCR cloning of cDNA using the following primers: *lacZ*: 5'-GGAGGATCCGAATCTCTATCGTGCGGTG-3', 5'-GCGCAAGCTTGTAAACGCCTCGAATCAGCAAC-3'; *Pax5*: 5'-GAGGGATCCCTGCTTGGCTCCCCATACTAT-3', 5'-CCCAGCTTAGCCAGAAGTCAGATGCTCA-3';

Pax2: 5'-GGAGGATCCGAGTCGGAGGCTTCGCTGGAG-3',
5'-CCACAAGCTTCCGACCCTTGCCTCCAGTG-3'.

RESULTS

Insertion of a *Pax5* minigene into the *Pax2* locus

The Pax5 protein is collinear with Pax2b, the major isoform encoded by the *Pax2* gene (Adams et al., 1992; Dressler and Douglass, 1992). Moreover, the equivalent exons 2 of *Pax2* and *Pax5* code for identical paired domain sequences and share a common *NcoI* site. We therefore fused the mouse *Pax5* cDNA at this *NcoI* site to *Pax2* to generate a *Pax5* minigene, which is expressed under the control of the *Pax2* locus (Fig. 1A). The expected fusion protein differs from the endogenous Pax5 protein only at five amino acid positions within its N-terminal sequence, which lacks any function and is encoded by *Pax2* exon 1 (see legend to Fig. 1A). The targeting vector additionally had the following features. The *Pax5* cDNA and the selection cassette consisting of the *tk* and *neo* genes were flanked by *loxP* sites, which facilitated subsequent deletion of these sequences by Cre recombinase (Fig. 1A). To be able to monitor deletion in vivo, we inserted a *lacZ* gene with its own 3' splice site downstream of the *tk* and *neo* genes. Upon Cre-mediated deletion, these *lacZ* sequences should be brought into the position of the deleted *Pax5* cDNA and thus be spliced at the mRNA level onto exon 1 sequences (Fig. 1A). The *Pax2^{lacZ}* allele should furthermore correspond to a null allele, as it is unable to code for a functional Pax2 protein (Fig. 1A).

Correctly targeted ES cells lacking the *tk* and *neo* selection

cassette were injected into blastocysts to generate heterozygous *Pax2^{5ki/+}* mice (Fig. 1B). These mice were crossed with a *nestin-cre* transgenic line (Betz et al., 1996) to obtain *Pax2^{+/-}* mice by Cre-mediated deletion of the *Pax5* minigene in the germline. The *Pax2^{5ki}* and *Pax2^{lacZ}* alleles were subsequently back-crossed for five generations into the C3H/He strain background.

Expression of the *Pax2^{lacZ}* and *Pax2^{5ki}* alleles

The expression of the *Pax2^{lacZ}* gene was analyzed by β -galactosidase staining of *Pax2^{+/-}* embryos at days 8.5-11.5 (Fig. 2A-C). β -galactosidase activity was detected in all the previously described *Pax2* expression domains, i.e. in the optic stalk, otic vesicle, spinal cord, developing kidney and at the MHB (Dressler et al., 1990; Nornes et al., 1990; Püschel et al., 1992). Hence, we conclude that the targeted *Pax2^{lacZ}* allele is expressed like the endogenous *Pax2* gene in heterozygous embryos.

We next investigated expression of the *Pax2^{5ki}* allele by RNase protection analysis of kidney RNA, which was isolated from *Pax2^{5ki/+}* and *Pax2^{5ki/5ki}* embryos at day 18.5. Riboprobes detecting the *Pax2*, *Pax5* and *lacZ* transcripts were used individually or in combination for the RNase protection experiment shown in Fig. 3A. Surprisingly, the *Pax2^{5ki/+}* kidney expressed the *Pax5* transcript of the *Pax2^{5ki}* allele at a lower level than the *Pax2* mRNA of the wild-type allele. Moreover, even the *lacZ* transcript could be detected, indicating that exon skipping of the primary *Pax2^{5ki}* transcript can occur by directly splicing *Pax2* exon 1 to the downstream *lacZ* sequences (Fig. 3A). Quantitation and normalization of

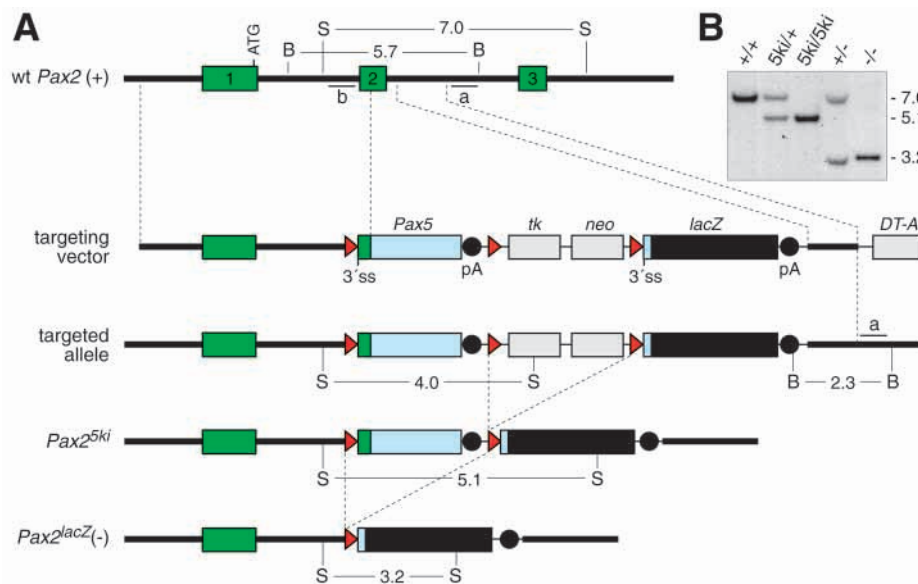
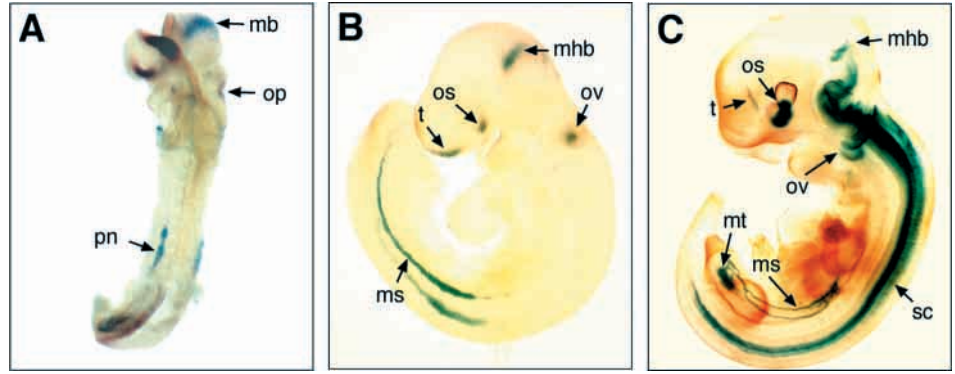


Fig. 1. Insertion of a *Pax5* minigene into the *Pax2* locus. (A) Structure of the wild-type and targeted *Pax2* loci. The murine *Pax5* cDNA was fused at a common *NcoI* site to *Pax2* exon 2 and linked at the 3' side to the trailer, polyadenylation (pA) and termination sequences of the rabbit β -globin gene. The downstream *lacZ* gene contains the 3' splice site (3'ss) of *Pax5* exon 2. The neomycin (*neo*) resistance and herpes simplex virus thymidine kinase (*tk*) genes were flanked by *loxP* sites (red arrowheads), to be deleted by transient Cre expression prior to injection of the targeted ES cells into mouse blastocysts. The *Pax2^{lacZ}* allele was generated by Cre-mediated deletion of the *Pax5* cDNA in the germline of *Pax2^{5ki/+}* mice. Correct targeting was verified by *BsmI* (B) and *SacI* (S) digestion of genomic DNA followed by Southern blot analysis with probes 'a' and 'b', respectively. The lengths of the respective DNA fragments are indicated in kb. The fusion protein encoded by the *Pax2^{5ki}* allele contains the N-terminal sequence of *Pax2* exon 1 (MDMHCKADPFSAMH) (Dressler et al., 1990), which differs at five positions from the corresponding Pax5 sequence (MEIHCKHDPFASMH) (Busslinger et al., 1996). DT-A, diphtheria toxin A gene. (B) Southern blot analysis. Tail DNA from mice of the indicated genotypes was digested with *SacI* and subjected to Southern blot analysis with probe 'b'.

Fig. 2. Expression of the *Pax2^{lacZ}* allele. (A) *Pax2^{+/-}* embryos were analyzed by β -galactosidase staining at day 8.5 (10 somites; A), 9.5 (B) and 11.5 (C). At day 8.5 (A), β -galactosidase expression is detected in the prospective midbrain (mb) region, otic placode (op) and pronephros (pn), at day 9.5 (B) in the telencephalon (t), optic stalk (os), otic vesicle (ov), mesonephric duct (ms) and at the midbrain-hindbrain boundary (mhb) and at day 11.5 (C) additionally in the spinal cord (sc) and metanephros (mt).



the RNase-protected signals to the control mRNA of the ribosomal *S16* gene indicated that the *Pax5* transcript of the *Pax2^{5ki}* allele was approx. fivefold less abundant than the *Pax2* mRNA of the wild-type allele in heterozygous kidneys (Fig. 3B). The *Pax2^{5ki}* allele furthermore gave rise to approx. threefold higher levels of the *lacZ* transcript compared to the *Pax5* mRNA. Western blot analysis revealed a similar situation at the protein level, as less Pax5 protein was detected in the *Pax2^{5ki/5ki}* kidney compared to the Pax2 protein in the wild-type kidney (Fig. 3C). As predicted by the RNase protection results, *Pax2^{5ki/5ki}* embryos expressed β -galactosidase activity in all *Pax2* expression domains (Fig. 3D). Hence, the observed exon skipping is not restricted to the kidney but instead is a general property of the *Pax2^{5ki}* allele.

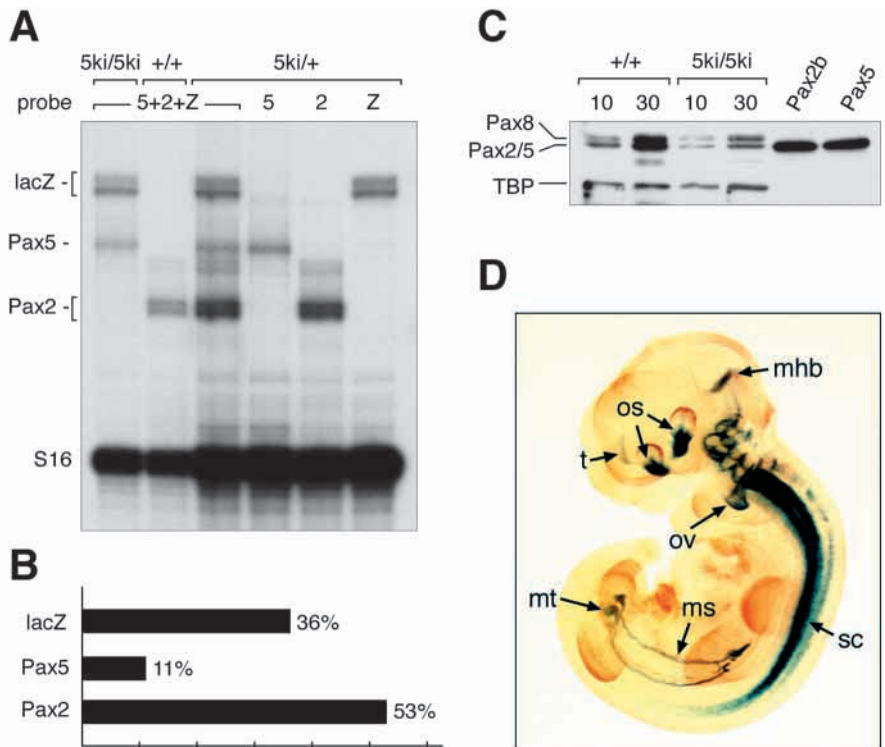
Normal midbrain and cerebellum development in *Pax2^{5ki}* mutant embryos

At day 8 of mouse embryogenesis, an organizing center is established at the midbrain-hindbrain boundary (MHB) that specifies patterning of the posterior midbrain and cerebellum

(reviewed by Wassef and Joyner, 1997). *Pax2* transcription is already initiated at day 7.5 in this embryonic brain region, whereas *Pax5* expression is activated only later at the 3- to 5-somite stage (Urbánek et al., 1994; Rowitch and McMahon, 1995). Hence, *Pax2* is the only member of the *Pax2/5/8* family that is expressed in the prospective MHB region between day 7.5 and 8.25. This short period is, however, critical for establishing the MHB organizer, since the midbrain and cerebellum fail to develop in *Pax2^{-/-}* embryos on the C3H/He background (Fig. 4C,F,I; Favor et al., 1996) in contrast to the minor patterning defects observed in *Pax5^{-/-}* mice (Urbánek et al., 1994).

To assess whether Pax5 can substitute for Pax2 during this critical time window, we analyzed the morphology of the developing midbrain and cerebellum in *Pax2^{5ki/5ki}* embryos at days 12.5 (Fig. 4B) and 18.5 (Fig. 4E,H). Inspection of the whole brain as well as examination of histological sections failed to reveal any morphological abnormality compared to wild-type embryos (Fig. 4A,D,G). The isthmic constriction was normally formed at the MHB of *Pax2^{5ki/5ki}* embryos and

Fig. 3. Exon skipping by alternative splicing of *Pax2^{5ki}* transcripts. (A) RNase protection analysis. Total RNA isolated from 18.5-day-old kidneys was analyzed with individual or combined *Pax2* (2), *Pax5* (5) and *lacZ* (Z) riboprobes. The *S16* transcript was comapped as control RNA. (B) Quantitation of the RNase protection data. The signals obtained with *Pax2^{5ki/+}* kidney RNA were quantitated by phosphorimager analysis, normalized for the number of incorporated radiolabeled G-residues and standardized to *S16* RNA. The level of each mRNA is shown as percentage relative to the sum of all the three mRNAs transcribed from the wild-type and targeted *Pax2* alleles. (C) Western blot analysis. Whole cell extracts (10 and 30 μ g of protein) of 18.5-day-old kidneys were analyzed by western blotting with monoclonal anti-TBP and polyclonal anti-paired domain antibodies (Adams et al., 1992). The reference Pax2b and Pax5 proteins were synthesized by coupled in vitro transcription/translation. (D) β -galactosidase staining of a *Pax2^{5ki/5ki}* embryo at day 11.5. β -galactosidase activity is detected in all *Pax2* expression domains.



was separated by a normal midbrain tectum from the posterior commissure, which consists of an array of transverse axon bundles demarcating the forebrain-midbrain boundary (Fig. 4B). The cerebellum also developed normally in *Pax2^{5ki/5ki}* embryos (Fig. 4E,H). In contrast, the isthmic constriction and midbrain tectum was missing in *Pax2^{-/-}* embryos, resulting in a caudal extension of the posterior commissure (Fig. 4C) (Schwarz et al., 1999) and loss of the posterior midbrain and cerebellum (Fig. 4F,I; Favor et al., 1996). These data unequivocally demonstrate that Pax5 can completely substitute for the critical Pax2 function at the onset of MHB development.

Normal morphogenesis of the inner ear in *Pax2^{5ki}* mutant embryos

We next investigated whether Pax5 can also replace Pax2 function during development of those organs (ear, eye and kidney) that never express the endogenous *Pax5* gene. The vertebrate inner ear develops from an epithelial thickening, the otic placode, which is located in proximity to the posterior hindbrain (Fig. 2A). Invagination of this placode gives rise to the otic vesicle, and later the otocyst, which differentiates into the ventral cochlea and dorsal vestibular apparatus of the inner ear (reviewed by Torres and Giráldez, 1998). *Pax2* expression

is initiated in the otic placode and then becomes restricted to the ventral region of the otic vesicle, which is known to generate the saccule, cochlea and spiral ganglia of the auditory nerve (Fig. 2; Nornes et al., 1990; Püschel et al., 1992). Consistent with this expression pattern, all three structures fail to form in the *Pax2^{-/-}* embryo, which instead contains an enlarged chamber at the ventral side of the inner ear. Development of the dorsal vestibular region encompassing the semicircular canals is, however, largely normal (Fig. 5D; Torres et al., 1996; Favor et al., 1996).

Histological examination at embryonic day 18.5 did not reveal any morphological abnormalities in the inner ear of *Pax2^{5ki/5ki}* embryos compared to wild-type embryos (Fig. 5A,B). The spiral ganglia, cochlea and its sensory organ of Corti consisting of inner and outer hair cells developed normally in *Pax2^{5ki/5ki}* embryos (Fig. 5A,B,E,F; data not shown). Moreover, both the saccule and utricle were properly formed in their usual size and location (Fig. 5A,B). These data therefore demonstrate that Pax5 can fully substitute for the Pax2 function in ear development.

Interestingly, a twofold reduction of *Pax5* expression in *Pax2^{5ki/-}* embryos resulted in enlargement and fusion of the utricle and saccule compartments at the expense of the cochlea (Fig. 5C). The cochlear canal was wider and markedly reduced in length (Fig. 5C), although the organ of Corti still developed normally (Fig. 5G). The ear phenotype of *Pax2^{5ki/-}* embryos is thus intermediate between the normal morphology of wild-type or *Pax2^{5ki/5ki}* embryos (Fig. 5A,B) and the severe *Pax2^{-/-}* phenotype, which is characterized by complete fusion of the utricle and saccule as well as by the absence of the cochlea (Fig. 5D). Hence, the analysis of *Pax2^{5ki/-}* embryos has uncovered a dependency of inner ear development on Pax protein dosage.

Rescue of eye development by the *Pax2^{5ki}* allele

The vertebrate eye develops via multiple inductive and morphogenetic processes from two principal components, the neuroectoderm and the overlying surface ectoderm which, upon induction, forms the lens. The initial out-pocketing of the neuroectoderm from the diencephalon generates the optic vesicle, which subsequently invaginates to generate a bilayered optic cup, giving rise to the neural and pigmented retina, and the optic stalk, later being transformed into the optic nerve (reviewed by Jean et al., 1998). The invagination of the retina leaves on the ventral side of the optic cup a transient cleft, the optic fissure, which further extends as a groove along the optic stalk. Vascularization of the retina occurs through this optic fissure, which later closes to form a uniform retina

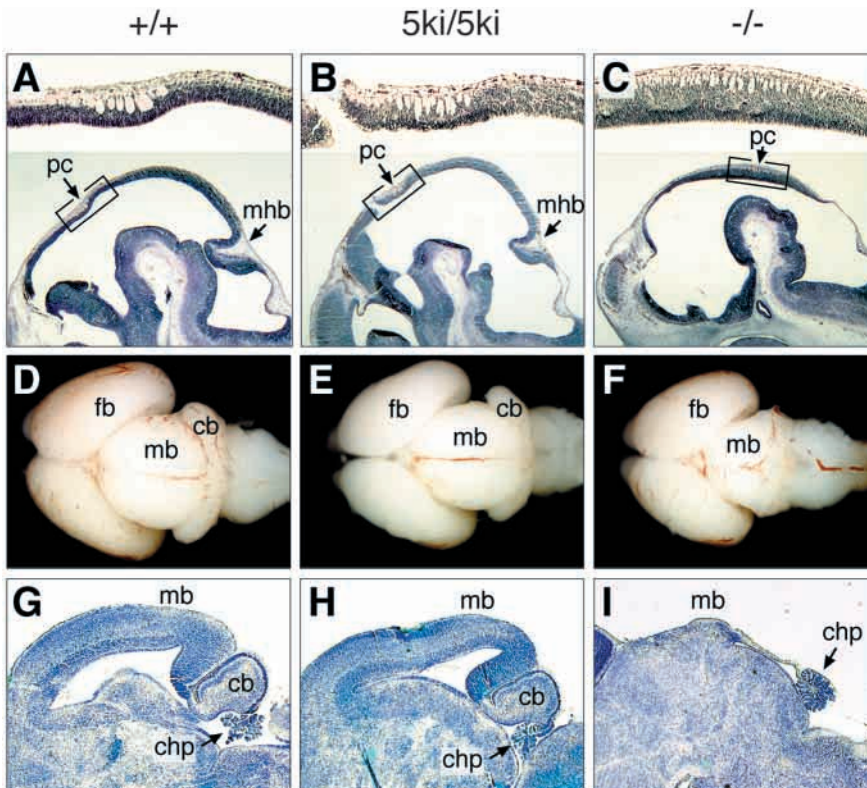


Fig. 4. Brain development in *Pax2^{5ki}* mutant embryos. The brains of *Pax2^{+/+}* (A,D,G), *Pax2^{5ki/5ki}* (B,E,H) and *Pax2^{-/-}* (C,F,I) embryos on the C3H/He strain background were compared at day 12.5 on sagittal sections stained with Eosin and Hematoxylin (A-C) and at day 18.5 in dorsal views of the whole brain (D-F) and on Nissl-stained sagittal sections (G-I). The morphology of the brain of *Pax2^{5ki/5ki}* embryos appears normal in all aspects (B,E,H). In contrast, the posterior commissure (pc) is shifted caudally and the midbrain-hindbrain boundary (mhb) region is missing in *Pax2^{-/-}* embryos (C), which fail to develop a posterior midbrain (mb) and cerebellum (cb) (F,I). chp, choroid plexus; fb, forebrain.

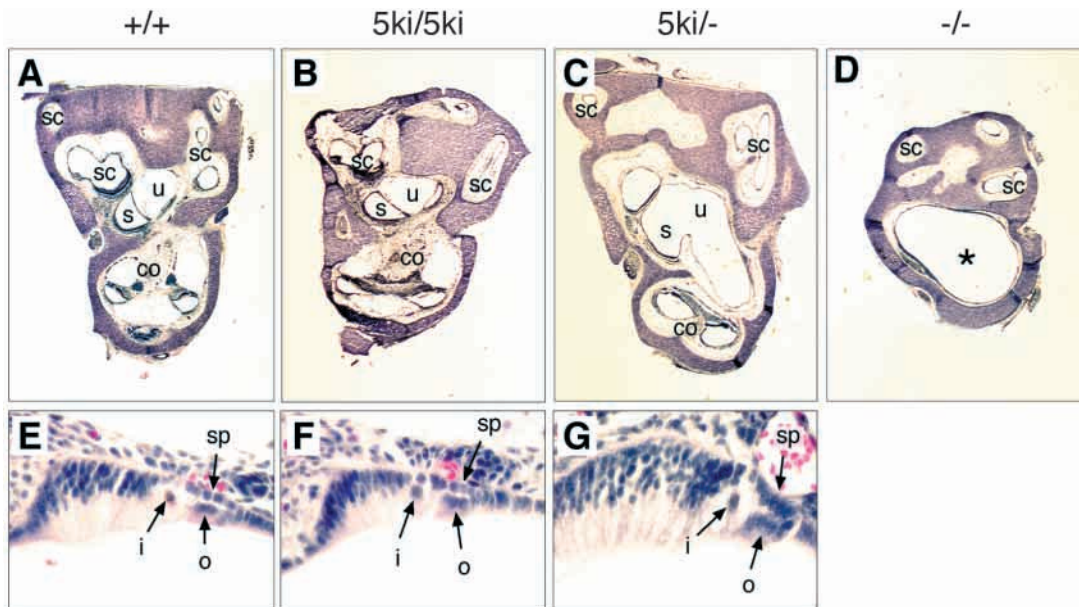


Fig. 5. Development of the inner ear in *Pax2*^{5ki} mutant embryos. The inner ear was dissected from *Pax2*^{+/+} (A,E), *Pax2*^{5ki/5ki} (B,F), *Pax2*^{5ki/-} (C,G) and *Pax2*^{-/-} (D) embryos at day 18.5 and analyzed on sagittal sections stained with Eosin and Hematoxylin. All structures of the wild-type ear (A) are also found in the inner ear of *Pax2*^{5ki/5ki} (B) and *Pax2*^{5ki/-} (C) embryos. The sensory organ of Corti, which consists of inner (i) hair, outer (o) hair and supporting (sp) cells, is normally formed within the cochlea (co) of all *Pax2*^{5ki} mutant embryos (E-G). The utricle (u) and saccule (s) are fused and enlarged in the *Pax2*^{5ki/-} ear, whereas the size of the cochlea is concomitantly reduced (C). The cochlea is entirely missing in the *Pax2*^{-/-} ear (D), which furthermore contains only one large chamber (asterisk) instead of the utricle and saccule. sc, semicircular canal.

(Silver and Robb, 1979). At embryonic day 9, *Pax2* expression is initiated in the optic vesicle, specifically within the region that later invaginates to form the optic cup. Subsequently, it is found in the ventral part of the optic cup on both sides of the optic fissure and along the entire optic stalk up to the diencephalon (Fig. 2; Nornes et al., 1990; Püschel et al., 1992; Otteson et al., 1998). *Pax2* expression is then excluded from all pigmented and neuroepithelial cells of the retina, thus forming a sharp boundary at the optic disc where the ganglion cell axons leave the retina and enter the optic nerve (Torres et al., 1996; Otteson et al., 1998). Consistent with this expression pattern, *Pax2* mutant embryos fail to close the optic fissure, exhibit severe abnormalities of optic disc and nerve formation and are unable to prevent pigmented retina cells from migrating into the optic stalk (Fig. 6D,H; Torres et al., 1996; Favor et al., 1996; Otteson et al., 1998).

To investigate the potential of *Pax5* to rescue this mutant eye phenotype, we compared dissected eyes and optic nerves of wild-type, *Pax2*^{5ki/5ki} and *Pax2*^{-/-} embryos at day 18.5. As shown in Fig. 6B, the optic fissure was closed in the eyes of all *Pax2*^{5ki/5ki} embryos analyzed, in marked contrast to *Pax2*^{-/-} embryos (Fig. 6D), indicating that *Pax5* can fully replace this *Pax2* function in eye morphogenesis. Closure of the optic fissure was even observed in *Pax2*^{5ki/-} embryos (Fig. 6C), indicating that this process requires only a minimal amount of *Pax* activity. Moreover, the extension of pigmented retina cells into the optic stalk was almost completely abolished in *Pax2*^{5ki/5ki} eyes compared to *Pax2*^{-/-} embryos (Fig. 6F,H). A few pigmented cells were, however, present in the nerve close to the optic disc (Fig. 6F). Cells of the pigmented retina extended further into the optic nerve in

Pax2^{5ki/-} eyes, although they were drastically reduced in number compared to *Pax2*^{-/-} eyes (Fig. 6G,H). Abnormalities ('scars') in the ventral region of the pigmented retina constitute yet another feature of the *Pax2*^{-/-} phenotype (Fig. 6D), which was never fully corrected in *Pax2*^{5ki/-} or *Pax2*^{5ki/5ki} eyes (Fig. 6B,C). We conclude therefore that the *Pax2*^{5ki} allele can rescue most but not all aspects of the *Pax2* mutant eye phenotype.

Development of normal genital tracts, but hypoplastic kidneys, in *Pax2*^{5ki} mutant embryos

Both the genital tracts and kidneys are derived by epithelial transformations from the intermediate mesoderm of the early embryo, which results in sequential development of the pronephros, mesonephros and metanephros. Whereas the pronephros is only a transient embryonic structure, the Wolffian duct of the mesonephros gives rise to the male genital tract consisting of the epididymis, vas deferens and seminal vesicle. In contrast, the Müllerian duct, another mesoderm-derived structure formed in parallel to the Wolffian duct, develops into the oviduct, uterus and part of the vagina of the female genital tract. Evagination of the ureteric bud from the posterior Wolffian duct is the first sign of metanephros development. Its invasion of the surrounding mesenchyme initiates an intensive phase of reciprocal inductive signaling, which results in formation of the glomeruli, tubules and collecting ducts of the adult kidney (reviewed by Saxén, 1987). The *Pax2* gene is expressed throughout development in mesenchymal and epithelial cells of the urogenital system. *Pax2* expression was thus observed in the Wolffian and Müllerian ducts as well as in the ureter, condensing mesenchyme, collecting ducts and differentiating nephrons of

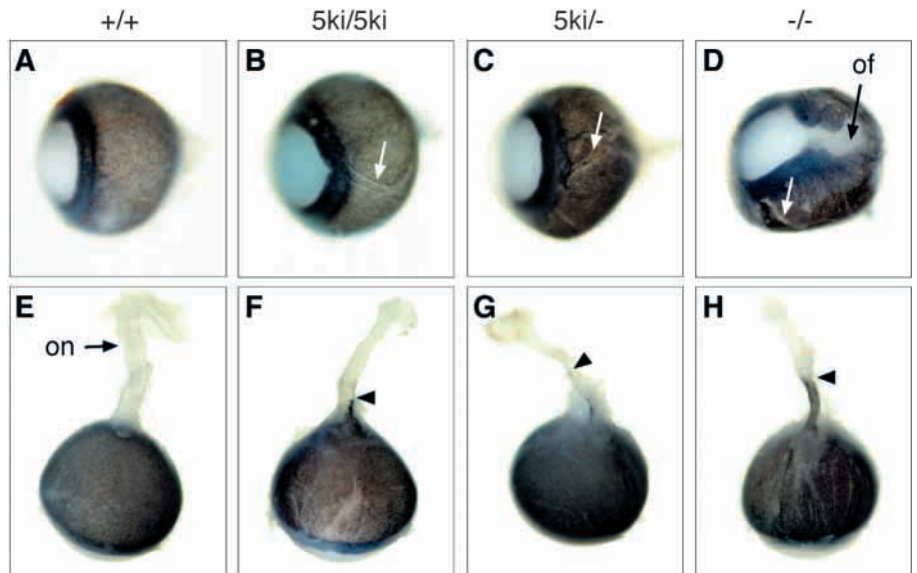


Fig. 6. Eye development in *Pax2*^{5ki} mutant embryos. The eyes together with the optic nerve (on) were dissected at day 18.5 from *Pax2*^{+/+} (A,E), *Pax2*^{5ki/5ki} (B,F), *Pax2*^{5ki/-} (C,G) and *Pax2*^{-/-} (D,H) embryos and photographed in ventral (A-D) and lateral (E-H) views. The optic fissure (of) failed to close in *Pax2*^{-/-} embryos (D), where cells of the pigmented retina expanded into the optic nerve (limit of migration denoted by arrowhead). Note the presence of malformations (scars, indicated by white arrows) in the ventral retina of *Pax2*^{5ki/5ki}, *Pax2*^{5ki/-} and *Pax2*^{-/-} embryos (B-D).

the metanephros (Fig. 2; Dressler et al., 1990; Torres et al., 1995). Embryos lacking *Pax2* initially form both the Wolffian and Müllerian ducts in the anterior region of the genital ridge (Torres et al., 1995); however, both ducts subsequently degenerate, resulting in the complete absence of genital tracts and kidneys, which is responsible for the perinatal lethality of *Pax2*^{-/-} mice (Fig. 7D,H; Torres et al., 1995; Favor et al., 1996).

To assess whether Pax5 can substitute for Pax2 during development of the urogenital systems, we dissected the kidneys and genital tracts of wild-type, *Pax2*^{5ki/5ki} and *Pax2*^{-/-} embryos at day 18.5. The metanephros was dramatically reduced in *Pax2*^{5ki/5ki} embryos of both sexes, ranging from 10% to 30% of the size of a wild-type kidney (Fig. 7A,B,E,F). The ureter was, however, normally formed in these embryos (Fig. 7B,F). In addition, the epididymis, vas deferens and seminal vesicle developed normally in male embryos (Fig. 7B; data not shown), as did the oviduct, uterus and vagina in female embryos (Fig. 7F; data not shown). The presence of all structures of the genital tract thus indicates that the Wolffian and Müllerian ducts are normally formed along their entire axis up to the cloaca in *Pax2*^{5ki/5ki} embryos, in marked contrast to *Pax2*^{-/-} embryos (Fig. 7D,H; Torres et al., 1995). We conclude, therefore, that Pax5 can fully replace the function of Pax2 in development of the genital tracts. The *Pax2*^{5ki} allele behaved, however, like a hypomorphic *Pax2* mutation in metanephros development, as it allowed formation of only small hypoplastic kidneys, which resulted in perinatal death of all *Pax2*^{5ki/5ki} mice due to renal failure.

Kidney development was more severely affected in *Pax2*^{5ki/-} embryos compared to *Pax2*^{5ki/5ki} embryos. The kidney was either formed only as a small remnant or was often totally absent together with the ureter (Fig. 7C,G). The male and female genital tracts, however, developed normally in these embryos (Fig. 7C,G), further indicating that distinct structures of the urogenital system require different Pax protein levels for their development.

Histological and immunohistochemical analyses at day 18.5 revealed that the *Pax2*^{5ki/5ki} embryos were able to form all

components of the metanephric kidney (Fig. 7I-L). The condensing mesenchyme around the ureteric tip, the comma- and S-shaped bodies, glomeruli, nephric tubules and collecting ducts were all present, although reduced in total number (Fig. 7J,L). This hypoplastic phenotype could be explained by a reduction in either cell proliferation or survival during *Pax2*^{5ki/5ki} kidney development. By analyzing the expression of phosphorylated histone H3 as a proliferation marker, we failed to observe any change in the proliferative index of *Pax2*^{5ki/5ki} kidneys relative to wild-type embryos at day 14.5 (Fig. 7M,N). In contrast, a significant increase of apoptotic cells was detected by TUNEL assay in *Pax2*^{5ki/5ki} kidneys compared to wild-type embryos (Fig. 7O,P). These data therefore suggest that increased apoptosis is responsible for the small size of *Pax2*^{5ki/5ki} kidneys, thus implicating Pax2 in the control of cell survival during metanephros development.

DISCUSSION

Functional equivalence of the Pax2 and Pax5 proteins in mouse development

The protein-coding sequences of *Pax2* and *Pax5* have been well conserved since their divergence from a common ancestral gene at the onset of vertebrate evolution (Pfeffer et al., 1998). In contrast, both genes have acquired radically different expression patterns, as they are to date coexpressed only in the developing CNS of the mouse embryo (Adams et al., 1992; Nornes et al., 1990). Consistent with this divergent regulation, gene targeting revealed an essential role of Pax2 in the development of the midbrain, cerebellum, eye, ear, kidney and genital tracts (Torres et al., 1995, 1996; Favor et al., 1996), whereas Pax5 fulfils an important function in B-lymphopoiesis (Urbánek et al., 1994; Nutt et al., 1999). By generating a mouse containing a *Pax5* minigene insertion in the *Pax2* locus, we have now demonstrated that the *Pax2*^{5ki} knock-in allele can rescue almost all aspects of the *Pax2* mutant phenotype. The midbrain, cerebellum, ear and genital tracts are normally formed in *Pax2*^{5ki/5ki} embryos, and even development of the

kidney and eye is largely restored by the *Pax2^{5ki}* allele. These data therefore indicate that the transcription factors Pax2 and Pax5 are able to regulate the same sets of target genes during mouse embryogenesis. This conclusion is further supported by structure-function analyses demonstrating that both proteins possess similar, if not identical, DNA-binding, transactivation

and repression functions (Kozmik et al., 1993; Dörfler and Busslinger, 1996; Lechner and Dressler, 1996; Czerny et al., 1997; Eberhard et al., 2000). This functional conservation is also reflected at the amino acid sequence level, as the Pax2b and Pax5 proteins share 98%, 53% and 77% sequence identity in the N-terminal paired domain, central sequences and C-

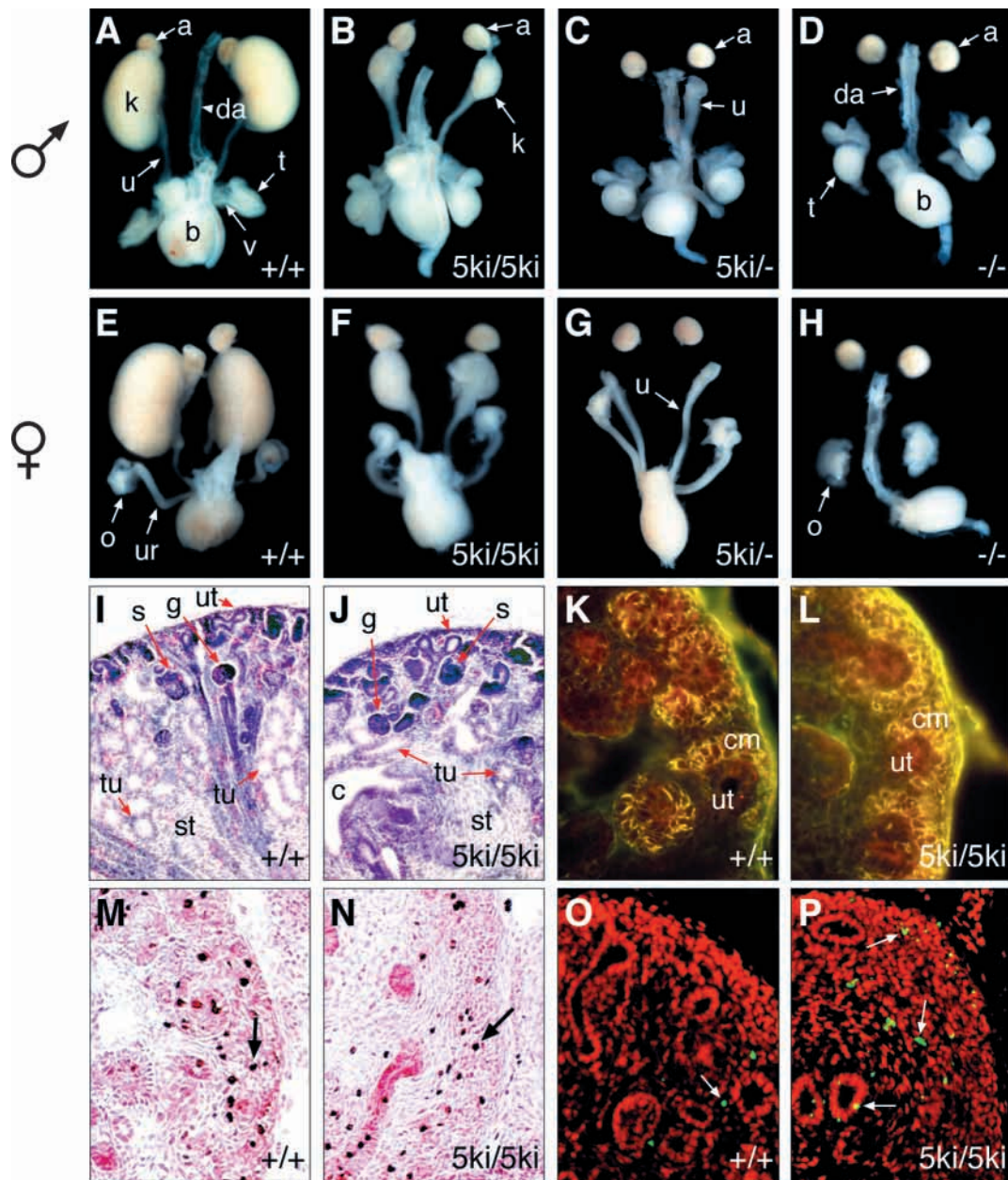


Fig. 7. Development of the urogenital system in *Pax2^{5ki}* mutant embryos. (A-H) The urogenital system of male (A-D) and female (E-H) 18.5-day embryos of the indicated genotypes was dissected and photographed. (I,J) Histological sections revealed the presence of all the characteristic structures of the wild-type kidney also in the hypoplastic *Pax2^{5ki/5ki}* kidney. (K, L) Normal condensation of the mesenchyme around the ureteric tip in the *Pax2^{5ki/5ki}* kidney as revealed by E-cadherin immunostaining (red) of the ureter and N-CAM staining (green) of the condensing mesenchyme. (M,N) Staining with anti-phosphoH3 antibodies (black dots indicated by arrows) revealed similar proliferation indices in *Pax2^{+/+}* and *Pax2^{5ki/5ki}* kidneys at day 14.5. The sections were counterstained with Eosin. (O,P) Increased cell death in the *Pax2^{5ki/5ki}* kidney at day 14.5. Cells undergoing apoptosis (green and yellow dots indicated by arrows) were identified by TUNEL assay on DAPI-counterstained sections. The blue color of DAPI was artificially adjusted to red. a, adrenal gland; b, bladder; c, calyx; cm, condensing mesenchyme; da, dorsal aorta; g, glomerulus; k, kidney; o, ovary; s, S-shaped body; st, stroma; t, testis; tu, tubule; u, ureter; ut, ureteric tip; ur, uterus; v, vas deferens.

terminal transactivation region, respectively (Dressler et al., 1990; Adams et al., 1992). In summary, our data demonstrate that Pax2 and Pax5 have maintained equivalent biochemical functions since their early divergence in vertebrate evolution. Hence, the functional differences between Pax2 and Pax5 are determined by the divergent expression patterns of the two genes.

Dosage-dependent effects of the Pax2^{5ki} allele

Heterozygous mutation of the human PAX2 gene is the underlying cause of the renal-coloboma syndrome, which is characterized by optic nerve abnormalities and renal insufficiency due to small hypoplastic kidneys (Sanyanusin et al., 1995; Cunliffe et al., 1998). A similar haploinsufficient phenotype was observed in heterozygous Pax2 mutant mice, indicating that the development of the optic nerve and metanephros is critically dependent on the Pax2 expression level (Keller et al., 1994; Torres et al., 1995; Favor et al., 1996; Otteson et al., 1998). Optic nerve abnormalities and hypoplastic kidneys are also the two phenotypic traits, which could not be fully rescued in Pax2^{5ki/5ki} mouse. These two phenotypes can, however, be explained by our finding that the Pax5 minigene of the Pax2^{5ki} allele is expressed at a fivefold lower level than the wild-type Pax2 gene during mouse embryogenesis. This reduction of the Pax5 mRNA level is caused by efficient skipping of the Pax5-coding sequences, due to alternative splicing of the primary transcript to the downstream lacZ gene in the Pax2^{5ki} locus. Consequently, the Pax5 mRNA is expressed at a lower level (approx. 20%) in homozygous Pax2^{5ki/5ki} embryos than is the wild-type Pax2 mRNA (50%) in heterozygous Pax2^{+/-} embryos. This expression difference is also reflected by the more severe hypoplasia of Pax2^{5ki/5ki} kidneys (Fig. 7) compared to Pax2^{+/-} kidneys (Keller et al., 1994; Torres et al., 1995; Porteous et al., 2000). Hence, the correlation between gene expression and phenotype strongly suggests that the lower expression level rather than a different biochemical property of Pax5 is responsible for the optic nerve and kidney abnormalities seen in Pax2^{5ki/5ki} embryos.

The Pax2 gene is known to give rise, by alternative splicing, to distinct protein isoforms (Dressler and Douglass, 1992; Ward et al., 1994; Heller and Brändli, 1997). The Pax5 protein encoded by the Pax2^{5ki} allele is colinear with Pax2b, the most abundant of these splice variants (Dressler and Douglass, 1992), and therefore Pax2^{5ki/5ki} embryos express only the equivalent of this major isoform. Nevertheless, the Pax2^{5ki} allele is able to rescue most aspects of the Pax2 mutant phenotype, which argues against a functional significance of the minor Pax2 splice variants.

Pax2-dependent control of cell survival during metanephros development

Due to the reduced expression of the inserted Pax5 minigene, the Pax2^{5ki} allele behaves like a hypomorphic Pax2 mutation in kidney development. Morphogenesis of the mesonephros appears to be normal in Pax2^{5ki/5ki} embryos, as indicated by the normal formation of male genital tracts. Metanephros development is, however, severely affected, as these embryos are able to form only a small number of all the epithelial structures characteristic of the adult kidney. The small size of Pax2^{5ki/5ki} kidneys is, however, not the consequence of reduced

cell proliferation, but rather reflects an increase in apoptosis during metanephros development. Heterozygous Pax2^{+/-} mice have recently been shown to exhibit a similar, though less severe, kidney phenotype (Ostrom et al., 2000; Porteous et al., 2000). It appears therefore that a moderate reduction in Pax2 protein level enhances programmed cell death, which is known to occur even during normal kidney morphogenesis (Koseki et al., 1992; Coles et al., 1993). Hence, the transcription factor Pax2 is likely to control the expression of cell survival factors or anti-apoptotic regulators in the developing kidney. Other members of the Pax gene family have previously been implicated in the regulation of cell survival, which may reflect a common function of Pax transcription factors (Bernasconi et al., 1996; Nutt et al., 1998; Borycki et al., 1999). The related Pax5 protein was shown to indirectly upregulate the expression of the antiapoptotic *bcl-xL* gene during B-lymphopoiesis (Nutt et al., 1998). Likewise, quantitative RT-PCR analysis revealed a significant reduction of *bcl-2* mRNA in the Pax2^{5ki/5ki} kidney (M. Bouchard, unpublished data). Interestingly, the kidney-specific expression of *bcl-2* is under the control of the transcription factor WT1 (Mayo et al., 1999), which itself is considered to be a target of Pax2 (Dehbi et al., 1996). Hence, Pax2 appears to indirectly regulate the *bcl-2* gene during kidney morphogenesis.

Pax gene function in midbrain and cerebellum development

Pax2 and Pax5 are coexpressed at the MHB of the mouse embryo, although with different spatiotemporal patterns. Transcription of the Pax2 gene is already initiated in this embryonic brain region during gastrulation (at day 7.5), whereas Pax5 expression is first observed at the 3- to 5-somite stage (at day 8.25) (Urbánek et al., 1994; Rowitch and McMahon, 1995). This difference in timing defines a period of 0.75 day, during which only Pax2 is expressed in the prospective MHB region. This time period is important for the development of the midbrain and cerebellum, as both brain structures fail to develop in Pax2^{-/-} embryos on the C3H/He background (Favor et al., 1996) (this study) and yet exhibit only minor patterning defects in Pax5^{-/-} mice (Urbánek et al., 1994). During this time window, Pax2 is critically involved in the activation of the *Fgf8* gene (Schwarz et al., 1999; M. Bouchard, unpublished data), which codes for an essential component of the signaling center at the MHB (Meyers et al., 1998). Pax2 furthermore controls the initiation of Pax5 transcription by directly binding to the MHB-specific enhancer of Pax5 (Pfeffer et al., 2000). Our finding, that development of the midbrain and cerebellum is completely rescued in Pax2^{5ki/5ki} embryos, unequivocally demonstrates that the transcription factors Pax2 and Pax5 can fulfil identical functions during MHB development. The functional difference between the two genes is therefore entirely determined by their distinct onset of expression at the MHB. A similar situation has previously been described for the differentially expressed *En1* and *En2* genes, which were also shown by gene replacement to code for functionally equivalent transcription factors involved in midbrain and cerebellum development (Hanks et al., 1995). Functional equivalence was furthermore demonstrated for the transcription factors Otx1 and Otx2 (Suda et al., 1999) as well as for paralogous Hox proteins (Greer et al., 2000).

Surprisingly, the loss of Pax2 is compatible with normal development of the midbrain and cerebellum in C57BL/6 mice (Schwarz et al., 1997), yet Pax2, Pax5 double-mutant embryos on the same genetic background fail to develop a posterior midbrain and cerebellum, which identifies Pax5 as the gene compensating for the lack of Pax2 (Schwarz et al., 1997). Our demonstration, that Pax2 and Pax5 are functionally equivalent transcription factors, suggests that differences in either the level and/or timing of Pax5 expression are responsible for the background-dependent phenotype of the Pax2 mutation. The dependency of Pax5 expression on Pax2 (Pfeffer et al., 2000) may be less stringent in the C57BL/6 embryo compared to the C3H/He strain, which would result in Pax5 expression even in Pax2 mutant embryos. The initiation of Pax5 expression could additionally be shifted to an earlier time point in C57BL/6 embryo, thus shortening the critical window between the onset of Pax2 and Pax5 expression at the MHB.

Unique functions of the vertebrate Pax2/5/8 genes by evolutionary divergence of cis-acting regulatory elements

The functional conservation of the Pax2 and Pax5 proteins entails that the vertebrate Pax2, Pax5 and Pax8 genes have diverged in function by the acquisition of different regulatory patterns. Interestingly, the single Pax258 gene of invertebrate chordates is expressed in embryonic structures that appear to be homologous to the expression domains of the vertebrate Pax2, Pax5 and Pax8 genes (Wada et al., 1998; Kozmik et al., 1999). Hence, the primordial Pax genes, which arose by gene duplications at the onset of vertebrate evolution, may initially have shared an identical expression pattern. Selective deletion of individual tissue-specific enhancers could subsequently have established a unique expression pattern for each of the three Pax2/5/8 genes during vertebrate evolution. This hypothesis is supported by the fact that Pax5 is still expressed during ear development of two lower vertebrates, the zebrafish (Pfeffer et al., 1998) and frog (Heller and Brändli, 1999), in marked contrast to the mouse (Urbánek et al., 1994). Hence, the Pax5 gene seems to have lost its ear-specific regulatory element only in the mammalian lineage. Moreover, Pax8 is still coexpressed together with Pax2 during eye development of the zebrafish in contrast to the frog and mouse (Pfeffer et al., 1998). Pax8 is known to be a key regulator of thyroid development in the mouse (Mansouri et al., 1998). Surprisingly, however, Pax2 instead of Pax8 is expressed in the developing thyroid gland of the frog (Heller and Brändli, 1999), thus further supporting the notion that all three members of the vertebrate Pax2/5/8 family are functionally equivalent transcription factors.

We thank H. Cremer for providing E14.1 ES cells. C. Theußl for blastocyst injection and G. Schaffner for DNA sequencing. This work was supported by the IMP and the Austrian Science Fund (grant P13601-GEN).

REFERENCES

Adams, B., Dörfler, P., Aguzzi, A., Kozmik, Z., Urbánek, P., Maurer-Fogy, I. and Busslinger, M. (1992). Pax-5 encodes the transcription factor BSAP and is expressed in B lymphocytes, the developing CNS, and adult testis. *Genes Dev.* **6**, 1589-1607.

Asano, M. and Gruss, P. (1992). Pax-5 is expressed at the midbrain-hindbrain boundary during mouse development. *Mech. Dev.* **39**, 29-39.

Bernasconi, M., Remppis, A., Fredericks, W. J., Rauscher III, F. J. and Schäfer, B. W. (1996). Induction of apoptosis in rhabdomyosarcoma cells through down-regulation of PAX proteins. *Proc. Natl. Acad. Sci. USA* **93**, 13164-13169.

Betz, U. A. K., Voßhenrich, C. A. J., Rajewsky, K. and Müller, W. (1996). Bypass of lethality with mosaic mice generated by Cre-loxP-mediated recombination. *Curr. Biol.* **6**, 1307-1316.

Borycki, A.-G., Li, J., Jin, F., Emerson Jr, C. P. and Epstein, J. A. (1999). Pax3 functions in cell survival and in *pax7* regulation. *Development* **126**, 1665-1674.

Busslinger, M., Kliks, N., Pfeffer, P., Graninger, P. G. and Kozmik, Z. (1996). Deregulation of PAX-5 by translocation of the Eµ enhancer of the IgH locus adjacent to two alternative PAX-5 promoters in a diffuse large-cell lymphoma. *Proc. Natl. Acad. Sci. USA* **93**, 6129-6134.

Coles, H. S., Burne, J. F. and Raff, M. C. (1993). Large-scale normal cell death in the developing rat kidney and its reduction by epidermal growth factor. *Development* **118**, 777-784.

Cunliffe, H. E., McNoe, L. A., Ward, T. A., Devriendt, K., Brunner, H. G. and Eccles, M. R. (1998). The prevalence of PAX2 mutations in patients with isolated colobomas or colobomas associated with urogenital anomalies. *J. Med. Genet.* **35**, 806-812.

Czerny, T., Bouchard, M., Kozmik, Z. and Busslinger, M. (1997). The characterization of novel Pax genes of the sea urchin and *Drosophila* reveal an ancient evolutionary origin of the Pax2/5/8 family. *Mech. Dev.* **67**, 179-192.

Dehbi, M., Ghahremani, M., Lechner, M., Dressler, G. and Pelletier, J. (1996). The paired-box transcription factor, PAX2, positively modulates expression of the Wilms' tumor suppressor gene (WT1). *Oncogene* **13**, 447-453.

Dörfler, P. and Busslinger, M. (1996). C-terminal activating and inhibitory domains determine the transactivation potential of BSAP (Pax-5), Pax-2 and Pax-8. *EMBO J.* **15**, 1971-1982.

Dressler, G. R., Deutsch, U., Chowdhury, K., Nornes, H. O. and Gruss, P. (1990). Pax2, a new murine paired-box-containing gene and its expression in the developing excretory system. *Development* **109**, 787-795.

Dressler, G. R. and Douglass, E. C. (1992). Pax-2 is a DNA-binding protein expressed in embryonic kidney and Wilms tumor. *Proc. Natl. Acad. Sci. USA* **89**, 1179-1183.

Eberhard, D. and Busslinger, M. (1999). The partial homeodomain of the transcription factor Pax-5 (BSAP) is an interaction motif for the retinoblastoma and TATA-binding proteins. *Cancer Res.* **59**, 1716s-1724s.

Eberhard, D., Jiménez, G., Heavey, B. and Busslinger, M. (2000). Transcriptional repression by Pax5 (BSAP) through interaction with corepressors of the Groucho family. *EMBO J.* **19**, 2292-2303.

Favor, J., Sandulache, R., Neuhauser-Klaus, A., Pretsch, W., Chatterjee, B., Senft, E., Wurst, W., Blanquet, V., Grimes, P., Spörle, R. and Schughart, K. (1996). The mouse Pax2^{1Neu} mutation is identical to a human PAX2 mutation in a family with renal-coloboma syndrome and results in developmental defects of the brain, ear, eye, and kidney. *Proc. Natl. Acad. Sci. USA* **93**, 13870-13875.

Fu, W. and Noll, M. (1997). The Pax2 homolog *sparkling* is required for development of cone and pigment cells in the *Drosophila* eye. *Genes Dev.* **11**, 2066-2078.

Greer, J. M., Puetz, J., Thomas, K. R. and Capecchi, M. R. (2000). Maintenance of functional equivalence during paralogous Hox gene evolution. *Nature* **403**, 661-664.

Hanks, M., Wurst, W., Anson-Cartwright, L., Auerbach, A. B. and Joyner, A. L. (1995). Rescue of the *En-1* mutant phenotype by replacement of *En-1* with *En-2*. *Science* **269**, 679-682.

Heller, N. and Brändli, A. W. (1997). *Xenopus* Pax-2 displays multiple splice forms during embryogenesis and pronephric kidney development. *Mech. Dev.* **69**, 83-104.

Heller, N. and Brändli, A. W. (1999). *Xenopus* Pax-2/5/8 orthologues: novel insights into Pax gene evolution and identification of Pax-8 as the earliest marker of otic and pronephric cell lineages. *Dev. Genet.* **24**, 208-219.

Jean, D., Ewan, K. and Gruss, P. (1998). Molecular regulators involved in vertebrate eye development. *Mech. Dev.* **76**, 3-18.

Keller, S. A., Jones, J. M., Boyle, A., Barrow, L. L., Killen, P. D., Green, D. G., Kapousta, N. V., Hitchcock, P. F., Swank, R. T. and Meisler, M. H. (1994). Kidney and retinal defects (*Krd*), a transgene-induced mutation with a deletion of mouse chromosome 19 that includes the Pax2 locus. *Genomics* **23**, 309-320.

- Koseki, C., Herzlinger, D. and al-Awqati, Q.** (1992). Apoptosis in metanephric development. *J. Cell Biol.* **119**, 1327-1333.
- Kozmik, Z., Kurzbauer, R., Dörfler, P. and Busslinger, M.** (1993). Alternative splicing of *Pax-8* gene transcripts is developmentally regulated and generates isoforms with different transactivation properties. *Mol. Cell. Biol.* **13**, 6024-6035.
- Kozmik, Z., Holland, N. D., Kalousova, A., Paces, J., Schubert, M. and Holland, L. Z.** (1999). Characterization of an amphioxus paired box gene, *AmphiPax2/5/8*: developmental expression patterns in optic support cells, nephridium, thyroid-like structures and pharyngeal gill slits, but not in the midbrain-hindbrain boundary region. *Development* **126**, 1295-1304.
- Lechner, M. S. and Dressler, G. R.** (1996). Mapping of Pax-2 transcription activation domains. *J. Biol. Chem.* **271**, 21088-21093.
- Mansouri, A., Hallonet, M. and Gruss, P.** (1996). Pax genes and their roles in cell differentiation and development. *Curr. Opin. Cell Biol.* **8**, 851-857.
- Mansouri, A., Chowdhury, K. and Gruss, P.** (1998). Follicular cells of the thyroid gland require *Pax8* gene function. *Nature Genet.* **19**, 87-90.
- Matisse, M. P. and Joyner, A. L.** (1997). Expression patterns of developmental control genes in normal and *engrailed-1* mutant mouse spinal cord revealed early diversity in developing interneurons. *J. Neurosci.* **17**, 7805-7816.
- Mayo, M. W., Wang, C.-Y., Drouin, S. S., Madrid, L. V., Marshall, A. F., Reed, J. C., Weissman, B. E. and Baldwin, A. S.** (1999). WT1 modulates apoptosis by transcriptionally upregulating the *bcl-2* proto-oncogene. *EMBO J.* **18**, 3990-4003.
- Meyers, E. N., Lewandoski, M. and Martin, G. R.** (1998). An *Fgf8* mutant allelic series generated by Cre- and Flp-mediated recombination. *Nature Genet.* **18**, 136-141.
- Noll, M.** (1993). Evolution and role of Pax genes. *Curr. Opin. Genet. Dev.* **3**, 595-605.
- Nornes, H. O., Dressler, G. R., Knapik, E. W., Deutsch, U. and Gruss, P.** (1990). Spatially and temporally restricted expression of Pax2 during murine neurogenesis. *Development* **109**, 797-809.
- Nutt, S. L., Morrison, A. M., Dörfler, P., Rolink, A. and Busslinger, M.** (1998). Identification of BSAP (Pax-5) target genes in early B-cell development by loss- and gain-of-function experiments. *EMBO J.* **17**, 2319-2333.
- Nutt, S. L., Heavey, B., Rolink, A. G. and Busslinger, M.** (1999). Commitment to the B-lymphoid lineage depends on the transcription factor Pax5. *Nature* **401**, 556-562.
- Ostrom, L., Tang, M. J., Gruss, P. and Dressler, G. R.** (2000). Reduced *Pax2* gene dosage increases apoptosis and slows the progression of renal cystic disease. *Dev. Biol.* **219**, 250-258.
- Otteson, D. C., Shelden, E., Jones, J. M., Kameoka, J. and Hitchcock, P. F.** (1998). Pax2 expression and retinal morphogenesis in the normal and *Krd* mouse. *Dev. Biol.* **193**, 209-224.
- Pfeffer, P. L., Gerster, T., Lun, K., Brand, M. and Busslinger, M.** (1998). Characterization of three novel members of the zebrafish *Pax2/5/8* family: dependency of *Pax5* and *Pax8* expression on the *Pax2.1 (noi)* function. *Development* **125**, 3063-3074.
- Pfeffer, P. L., Bouchard, M. and Busslinger, M.** (2000). Pax2 and homeodomain proteins regulate a 435 bp enhancer of the mouse *Pax5* gene at the midbrain-hindbrain boundary. *Development* **127**, 1017-1028.
- Plachov, D., Chowdhury, K., Walther, C., Simon, D., Guenet, J. L. and Gruss, P.** (1990). *Pax8*, a murine paired box gene expressed in the developing excretory system and thyroid gland. *Development* **110**, 643-651.
- Porteous, S., Torban, E., Cho, N.-P., Cunliffe, H., Chua, L., McNoe, L., Ward, T., Souza, C., Gus, P., Giugliani, R., Sato, T., Yun, K., Favor, J., Sicotte, M., Goodyer, P. and Eccles, M.** (2000). Primary renal hypoplasia in humans and mice with *PAX2* mutations: evidence of increased apoptosis in fetal kidneys of *Pax2*^{1Neu +/-} mutant mice. *Hum. Mol. Genet.* **9**, 1-11.
- Püschel, A. W., Westerfield, M. and Dressler, G. R.** (1992). Comparative analysis of Pax-2 protein distributions during neurulation in mice and zebrafish. *Mech. Dev.* **38**, 197-208.
- Rowitch, D. H. and McMahon, A. P.** (1995). *Pax-2* expression in the murine neural plate precedes and encompasses the expression domains of *Wnt-1* and *En-1*. *Mech. Dev.* **52**, 3-8.
- Sanyanusin, P., Schimmenti, L. A., McNoe, L. A., Ward, T. A., Pierpont, M. E. M., Sullivan, M. J., Dobyns, W. B. and Eccles, M. R.** (1995). Mutation of the *PAX2* gene in a family with optic nerve colobomas, renal anomalies and vesicoureteral reflux. *Nature Genet.* **9**, 358-364.
- Saxén, L.** (1987). *Organogenesis of the Kidney*. Cambridge University Press.
- Schwarz, M., Alvarez-Bolado, G., Urbánek, P., Busslinger, M. and Gruss, P.** (1997). Conserved biological function between *Pax-2* and *Pax-5* in midbrain and cerebellum development: Evidence from targeted mutation. *Proc. Natl. Acad. Sci. USA* **94**, 14518-14523.
- Schwarz, M., Alvarez-Bolado, G., Dressler, G., Urbánek, P., Busslinger, M. and Gruss, P.** (1999). *Pax2/5* and *Pax6* subdivide the early neural tube into three domains. *Mech. Dev.* **82**, 29-39.
- Silver, J. and Robb, R. M.** (1979). Studies on the development of the eye cup and optical nerve in normal mice and in mutants with congenital optic nerve aplasia. *Dev. Biol.* **68**, 175-190.
- Suda, Y., Nakabayashi, J., Matsuo, I. and Aizawa, S.** (1999). Functional equivalency between *Otx2* and *Otx1* in development of the rostral head. *Development* **126**, 743-757.
- Torres, M., Gómez-Pardo, E., Dressler, G. R. and Gruss, P.** (1995). *Pax-2* controls multiple steps of urogenital development. *Development* **121**, 4057-4065.
- Torres, M., Gómez-Pardo, E. and Gruss, P.** (1996). *Pax2* contributes to inner ear patterning and optic nerve trajectory. *Development* **122**, 3381-3391.
- Torres, M. and Giráldez, F.** (1998). The development of the vertebrate inner ear. *Mech. Dev.* **71**, 5-21.
- Urbánek, P., Wang, Z.-Q., Fetka, I., Wagner, E. F. and Busslinger, M.** (1994). Complete block of early B cell differentiation and altered patterning of the posterior midbrain in mice lacking *Pax5/BSAP*. *Cell* **79**, 901-912.
- Urbánek, P., Fetka, I., Meisler, M. H. and Busslinger, M.** (1997). Cooperation of *Pax2* and *Pax5* in midbrain and cerebellum development. *Proc. Natl. Acad. Sci. USA* **94**, 5703-5708.
- Wada, H., Saiga, H., Satoh, N. and Holland, P. W. H.** (1998). Tripartite organization of the ancestral chrodate brain and the antiquity of placodes: insights from ascidian *Pax-2/5/8*, *Hox* and *Otx* genes. *Development* **125**, 1113-1122.
- Ward, T. A., Nebel, A., Reeve, A. E. and Eccles, M. R.** (1994). Alternative messenger RNA forms and open reading frames within an additional conserved region of the human *PAX-2* gene. *Cell Growth Diff.* **5**, 1015-1021.
- Wassef, M. and Joyner, A. L.** (1997). Early mesencephalon/metencephalon patterning and development of the cerebellum. *Persp. Dev. Neurobiol.* **5**, 3-16.